Annual Technical Report

on

# Earthquake Monitoring of the Hanford Region, Eastern Washington

Geophysics Program
University of Washington
Seattle, Washington 98195

July 15, 1977

PREPARED FOR THE U.S. ENERGY RESEARCH &
DEVELOPMENT ADM. UNDER CONTRACT NO.
E(45-1)-2225, TASK AGREEMENT NO. 39

TABLE OF CONTENTS



Report prepared by: Stephen D. Malone
206-543-7010

# Introduction

This report is for the fiscal year 1977 and includes the results of our routine operations and analysis for the Hanford seismic network as well as the results of specific studies which address the general problem of earthquake hazards in eastern Washington. The report is divided into several sections dealing with specific topics or investigations.

The routine operations of the network are reported on quarterly. We give here a summary of those reports with additional detail covering changes in the array configuration, operational problems we have had and an outline of changes and improvements to come. We next address the subject of regional seismicity and how it has changed or appeared to change since we took over the array operations in 1975. We include comments on our detectability and locatability thresholds and address the problem of uniformity of data. Since regional velocity structure is important to accurate hypocentral determination, we include a section on our work in this area. We have expanded the work reported in a preliminary report by Eaton to cover the northern half of the array. Of special interest to hazards evaluation is the section on magnitude and attenuation relations. We report on our development of a new coda-length magnitude relation and a progress report on our work on the seismic attenuation properties of the region. Two areas have been studied in detail during the past year. The data analysis from the Wooded Island swarm is nearly complete with interesting results as to the characteristics of the local velocity structure. An area of higher than normal seismicity south of Lake Chelan is being studied in some detail. Unlike the majority of the earthquakes in the Hanford region, these events appeared to be originating in the basement rocks below the basalt. Other sections deal with the ongoing tilt meter study and other special projects.

## Operations

During the fiscal year 1977 the extended Hanford seismic array has been in continuous operation. We estimate the amount of down time for a major part of the array to be about 9% of the time. These outages are due to record changing time, developer failure (film jam, chemical clog) and power failures. During these times events in the area could not be located; however, events up to about $M_L$ = 2 1/2 would be detected by helicorder records and neighboring arrays. There were no events within the array larger than $M_L$ = 2 1/2 which were not locatable.

Individual station outages have been an annoying problem requiring a good deal of technician time to remedy. We have had some problems with the USGS tube type VCO's center frequency drift. The majority of our problems have been with telemetry by the phone company. This has been a particularly severe problem in the area to the north serviced by General Telephone. An example of a day with more than the usual problems is given below in a note by our technician who was constantly on the telephone to the lease line trouble board trying to get the situation cleared up.

> June 23, 1977 - Carrier failure on line 4GD0971 during which no signals came in for 5 hours. When it came back up there was a grounding problem at Midway which caused excessive noise and the loss of three signals (MDW, GBL, WAH) for two days. Same day lost three signals on line 4GD9715 due to phone problems in Hanford reservation. Same day finally got vantage leg repaired on line 4KD0921 which had been down because of phone company work for over a day. (three hours of technician time spent dealing with these problems)

The loss of individual stations from time to time does not seriously affect our location ability for earthquakes greater than $M_L$ = 2.0 however does

require considerable effort to make sure the outages repaired rapidly.

During the past year several changes in the array configuration have taken place. Table1 lists the stations in eastern Washington used for locations. Figure 1 shows these stations and planned locations for new stations. During the past year the worldwide station at Newport, Washington has been added to the develecorder records. Stations at Waterville (WAT) and Entiat (ENT) were added by removing the horizontal components at ODS, and VTG. The station at Colville (COL) has been removed due to low seismicity and a noisy site.

New stations have been started as of July 1, 1977 at Plain near Lake Wenatchee (PLN) and Winthrop (WTH). A new site has been located for the Hermiston (HER) station 10 km to the west which should reduce the cultural noise there and improve the array geometry. New stations are planned in the central Cascades with support from WPPSS. Possible locations for several of these stations are shown on figure 1.

Table 1. Station Locations and Delays

| Name | Latitude | Longitude | L | South Delay | North Delay |
|---|---|---|---|---|---|
| MDW | 46 38 48.00 | 119 45 39.00 | | | .53 |
| SYR | 46 51 46.80 | 119 37 04.20 | | | .47 |
| OTH | 46 44 20.40 | 119 12 59.40 | | | .39 |
| WAH | 46 45 07.20 | 119 34 40.80 | | | .55 |
| CRF | 46 49 30.60 | 119 23 05.60 | | | .47 |
| GBL | 46 35 51.60 | 119 27 35.40 | | | .57 |
| ETP | 46 27 53.40 | 119 03 32.40 | | | .30 |
| BDG | 46 14 04.80 | 119 19 03.00 | | | .48 |
| EUK | 46 23 45.00 | 118 33 43.50 | | -.10 | .26 |
| PRO | 46 12 45.60 | 119 41 09.00 | | | .54 |
| RSW | 46 23 28.20 | 119 35 19.20 | | | .62 |
| PEN | 45 36 43.20 | 118 45 46.50 | | -.15 | .18 |
| WGW | 46 02 40.80 | 118 55 57.60 | | | .35 |
| WIW | 46 25 55.80 | 119 17 17.40 | | | .55 |
| HER | 45 50 08.40 | 119 22 51.00 | | | .47 |
| MFW | 45 54 10.80 | 118 24 21.00 | | -.15 | .18 |
| OMK | 48 28 49.20 | 119 33 39.00 | | -.12 | .23 |
| DYH | 47 57 37.80 | 119 46 09.60 | | -.20 | .07 |
| WBW | 48 01 04.20 | 119 08 13.80 | | -.22 | .11 |
| SAW | 47 42 06.00 | 119 24 03.60 | | -.25 | .06 |
| CBW | 47 48 25.50 | 120 01 57.60 | | -.30 | |
| FPW | 47 58 00.00 | 120 12 46.50 | | -.30 | |
| WEN | 47 31 46.20 | 120 11 39.00 | | -.30 | |
| EPH | 47 21 07.80 | 119 35 46.20 | | -.14 | .20 |
| ODS | 47 18 24.00 | 118 44 42.00 | | -.20 | .11 |
| DAV | 47 38 18.00 | 118 13 33.60 | | -.20 | .11 |
| WRD | 46 58 11.40 | 119 08 36.00 | | -.05 | .35 |
| WAT | 47 41 55.00 | 119 57 15.00 | | -.25 | .04 |
| ENT | 47 40 44.00 | 120 13 48.00 | | -.24 | .07 |
| VTG | 46 57 28.80 | 119 59 14.40 | | | .28 |
| COL | 48 35 36.00 | 117 52 55.20 | | | |
| NEW | 48 15 50.00 | 117 07 13.00 | | | |
| FMC | 45 37 28. | 120 01 42. | | -.20 | |
| RPK | 45 45 42. | 120 13 50. | | -.20 | |
| ALD | 45 49 10. | 120 04 00. | | -.20 | |

Under lined delays are from time term analysis

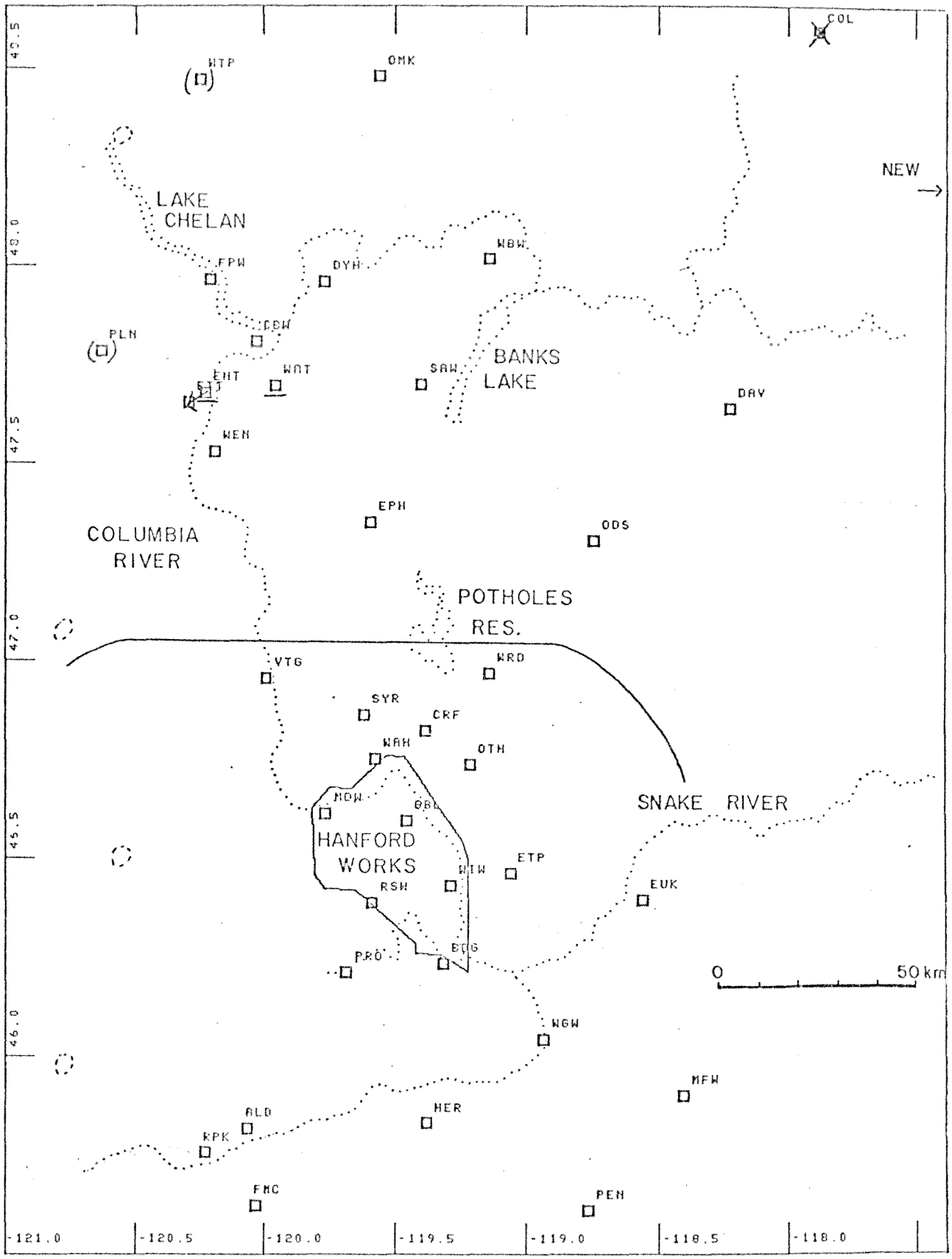


Figure 1a. Stations in the extended Hanford network operated by the University of Washington. COL marked X was discontinued in March, 1977. ENT and WAT were added in Dec. 1976. PLN and WTP were added July 1, 1977. Line divides north and south model areas.

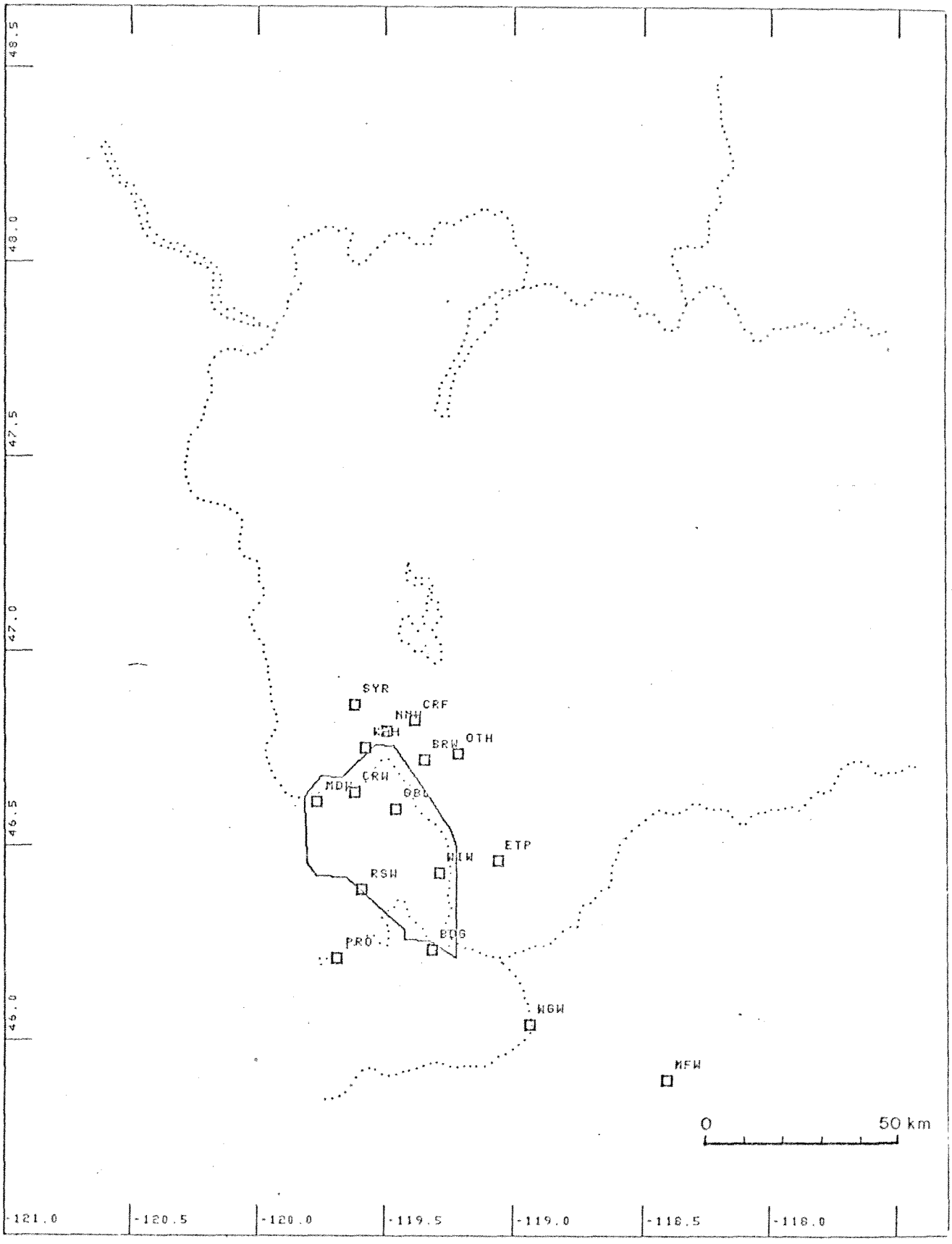


Figure 1b. Stations in the U.S. Geological Survey network as of 1975 when the University of Washington took over array operations.

## Seismicity

In this section we address the question of the seismicity level in eastern Washington, changes that may have occurred in the last seven years, and the uniformity of the existing data. Because two independent organizations operated the network, analysed the data and had different array configurations, it is difficult to obtain a uniform data set over the entire period. We attempt to address this problem and the implications of our interpretations in the following section.

We have obtained the final summary cards of the USGS locations from the Hanford area covering the period March 1969 - December 1974; however, we have not received their final report on their interpretations. With only limited information on the uniformity of their data as far as detectability, location biases and magnitude estimations, we can do nothing but accept their data set as complete, and unbiased. From personal communications, we understand that their method of computing magnitude changed sometime in 1971 and that the array configuration underwent several changes in the early years. We, therefore, know that their data set is not uniform though have no way of estimating how non-uniform it may be or in what specific way. We do address the problem of magnitude biases in a later section. For this section we used the USGS magnitudes as reported on their final summary cards.

For the University of Washington data all events previously reported have been reexamined for reading errors, the scanning sheets were gone over to detect any events missed by operator error, and blasts were searched for and flagged. All events were relocated using the new models and station corrections discussed in the structure section of this report. Magnitudes were recalculated using the new magnitude-coda length relation discussed elsewhere in this report.

A list of all analysed events from July 1, 1975 through March 31, 1976 is included in the appendix to this report. Punched summary cards are available to update anyone's data file who requests them.

To address the problem of the time stationarity of the seismicity in the immediate Hanford area, we have plotted all the earthquakes greater than $M_L$ = 1.6 for 12 month periods from 1969 to the present (Figure 2 ). Known and suspected blasts have been removed from the data. Since most major blasts are set off in the late afternoon, a histogram of number of events versus time of day should show a peak in the late afternoon if there were many blasts left in the data set. Figure 3 is such a plot for the data in Figure 2 . It shows that the events are distributed fairly uniformly in time and that the data should not be strongly contaminated with unidentified blasts. Because of major discontinuities in array geometry and operations techniques, we have selected the twelve month intervals such as to exclude periods of great change. The area chosen includes all events greater than $M_L$ = 1.6 for all array configurations including the present. We feel that fewevents of $M_L$ = 1.6 or greater would have been missed within this area since recording began. The number of events in magnitude categories are plotted in a histogram in Figure 4 . Note that the 12 month period in 1969-1970 has many more large events than any other period and fewer small events. We feel this is due to the different magnitude scale being used by the USGS duirng this time and does not represent a real change in seismic energy release. For the four years 1972-1975 there occurred an average of 40 events larger than $M_L$ = 1.6 each year and an average of 16 events larger than $M_L$ = 2. It appears 1973 was slightly below the average and the last 12 months, 76-77 is considerably below the average with only 12 events larger than $M_L$ = 1.6 occurring. We feel this is a real effect and represents a lull in seismic energy release in the Hanford area. The second quarter of 1977 is

presently being processed and appears to have more events coming from this area representing a return to more normal levels of seismicity. The presence or absence of swarms strongly influences the variability in time of the activity.

We next address the problem of the detectability and locatability of events in the eastern Washington area using the present array configuration. We have ascertained areas in eastern Washington where we are able to detect certain magnitude levels of earthquakes. To accomplish this, each station was analysed in the form of a distance-magnitude plot. An example is shown in Figure 5 . Each dot represents a located epicenter using that particular station along with at least three other stations. A line is drawn under the plotted points to reflect a distance-magnitude detectability under the most advantageous conditions for recording an earthquake at that station. These conditions may include the path traveled from epicenter to station, the particular earthquake mechanism, lack of noise at the recording site at the time of the recording, and the skill of the person scanning and picking signals off the channel from that station. It is therefore a best condition slope of detectability which we plot. The data used is from 1975 and 1976. The distances from each station for a magnitude 2.0 and 1.5 earthquake are used as a radius and a line was drawn outlining areas where four or more stations could see those magnitude earthquakes (see Figure 6 ).

Since these curves represent optimal conditions for detecting earthquakes, not all events larger than $M_L$ = 1.5 have been located within the inner curve. The rectangle centered on the Hanford area represents the area from which we feel all events larger than $M_L$ = 1.7 have been located based on the curvature of the log N versus M curve discussed in a later section. Based on a similar analysis of a larger area we feel that all events larger than $M_L$ = 2.0 have been located within the Mag 1.5 line on Figure 6 . Outside this line there

is no guarantee that any sized event will surely be located since the ability to obtain a converging hypocentral determination does not only depend on detectability when the event is located considerably outside the array boundaries. We do attempt to locate the larger events which fall outside the Mag 1.5 line though we can not say that all events have accurate epicenters.

To examine the regional seismic pattern for the last six years, we divide this time into three periods of roughly two years each and plot all events larger than $M_L$ = 2 in eastern Washington in Figure 7 . One must remember that the array is much larger for the last period shown and therefore the greater number of events outside the immediate Hanford area is an artifact of the array geometry. In Figure 8 we show all events greater than $M_L$ = 2.0 from 1969 to the present. The area of greatest activity is just north and northeast of the Hanford reservation and the area just south of Lake Chelan. There is a scattering of events to the west and a smaller group of events to the southwest. There appears to be no geographical association of these areas of higher seismicity and the major structural features in the area.

Since most of the events shown in Figure 8 are shallow events occurring within the basalt flows, they may not be representative of possible large regional structures capable of large events. We next examine the deeper events, those with depths greater than 8 km. Since there are few of these events, we drop our magnitude cut off to $M_L$ = 1.5 for the plot shown in Figure 9 . Based on the magnitude-frequency relation discussed in a later section, we expect 50% of the magnitude $M_L$ = 1.5 to be missing from this plot since they were not detected on enough stations to be well located. Events that lie outside the array boundaries have poor depth control; thus the deep events to the west of Hanford may not be well lcoated and may be misleading when looking at the whole area. The events to the south-southwest of Hanford are well located

and do represent a real concentration of deeper earthquakes. The larger of these events occurred in the second quarter of 1975 when the USGS was operating the net and the University of Washington processed the data. Because of problems with quality control we plan to reexamine these data to insure that the locations are good. The rest of the deep events appear to be scattered in similar areas as the shallow events with a hint of a line up north-south through the reservation. With additional stations to be installed this summer in the Cascades, better control on events to the west should be available.

## Velocity Structure

An accurate velocity model for an area is an important element in the ability to locate earthquakes accurately. Various investigations into the velocity structure in eastern Washington have been undertaken in the past. Published studies which have a direct bearing on our work are for example Hill (1972) and McCollom and Crosson (1975). As part of a preliminary report on the Hanford array operation by the USGS, Eaton did a time term analysis of explosions in the central Columbia Basin to examine the thickness of the crust and upper crustal basalt flows. This work and earlier work by Pitt (1971) provided the basis for the velocity model we have been using for routine analysis (Table 2 ). This model is almost identical to that used by the USGS for their routine analysis. Thus all hypocenters published by both ourselves and the USGS are based on essentially the same velocity model (Model A, Table 2 ), which is an attempt at averaging the lateral variations in structure over the central basin. The deeper layers are due to inferred velocity contrasts determined primarily from the Hill work (1972).

In this report we present additional work on the velocity structure investigations and a way of handling the gross lateral variations for hypocentral determinations. Since the array has been expanded to the north from the original USGS configuration it was imperative to do structural investigations in this area to compare with the better known area to the south. A modified time term method was used to investigate the basalt thickness north of 47°N. This method requires that the layers have only slowly varying thickness and the velocity be constant within a layer. We feel these criteria are fairly well met for the northern basin.

Five quarry sites were identified such that several shots were recorded

at each of the permanent stations. A relative time difference technique was used such that origin time was not needed. Arrivals were picked to within .01 sec and the standard error of the mean of several blasts at one station was typically .06 sec. The case for there being one dominant refractor which has first arrivals extending to at least 100 km was evident from several individual travel time curves. An example is shown in Figure 10 with lines fit by eye through the major arrivals. The transition to a velocity around 8.0 km/sec occurs at about a distance of 125 km, implying a crustal thickness of about 25 km.

The time term technique was used to investigate the delays or time terms associated with individual stations which lay along the approximately 6 km/sec refractor. The simultaneous inversion of the data from the five blast sites and 12 stations yield a refractor velocity of 6.05 $\pm$ .05 km/sec. The time terms for this inversion are given in Table 1 . These time terms may be converted to basalt thickness using 5.25 km/sec for the average basalt velocity. Figure 11 shows a north-south cross section of the basalt thickness (data for the central basin are from the preliminary report by Eaton). It appears to be one to two kilometers thick over most of the north-central basin though there are deviations in the time terms to indicate some roughness to the interface. For stations not on the basalt such as CBW and FPW the time terms are near zero. OMK, to the north, has a significant delay though the basalt is not present in this region. This delay is interpreted as a lateral variation in the basement rocks.

The results of this analysis and those of previous workers have been combined into a model for use in locating earthquakes through eastern Washington. Because there is such a large difference in the upper crustal structure between the Hanford region and the north central basin we have chosen to

divide all earthquakes in eastern Washington into two categories based on their approximate location. This is necessary since it is presently not possible to code into a computer location routine a laterally varying velocity structure. We have broken the region into two sections; one where the basalt is more than 4 km thick and another where it is less than 4 km thick. Figure 1 shows the division between these two areas as a heavy line and Table shows the appropriate velocity models. To the south and west we do not know the proper model and thus even though the basalt does not remain thick near the Cascade range we nevertheless use the thick basalt model for events in this area since the nearest stations are in such an area. We have also derived station delay terms to be used in the location routine to make up for the discrepancy between the known local velocity structure under a station and the average velocity model used for events in the region. Thus for an earthquake in the Hanford region, the "south" model would be used with a set of station delays which are generally negative for stations in the north. Conversely for events in the Chelan region the "north" model is used with station delays becoming more positive as you go south (Table 1 ).

We feel that this dual model location routine greatly increases the accuracy of locations, particularly for events to the north. For example, the average RMS value for several events in the Chelan area decreased by a factor of three when using the "north" model and its associated delays. The events reported on in the seismicity section of this report are the events since 1975 and have been relocated using this dual model system. All subsequent quarterly reports will use this technique for hypocentral determinations.

We anticipate minor adjustments to this model as stations are moved and more data become available; however, these changes will mostly be confined to the edges of the current array and should be of little influence on locations

within the current array. In particular, we hope to improve our knowledge of the crustal structure to the south and west. With additional stations in the Cascades we anticipate a better understanding of the crustal structure.

Detailed structure near the Hanford reservation. There is a need to know some of the detailed structure in the immediate vicinity of the Hanford reservation in particular the area of the Olympic-Wallula limament. The possibility exists that this large physiographic feature represents a structure on which a large earthquake could occur. To address this question information on the subsurface structure would be useful. It has been suggested that long seismic refraction lines be run across this area to attempt to obtain such information. We do not advocate such an approach for several reasons. Previous refraction work in the area suggests that major velocity changes within the basalt do not exist and thereofre the first major refraction arrival is from the basement rock beneath the basalt. From the Rattlesnake #1 well and Eaton's time term analysis it appears the basalt is quite thick in this area, more than 10 km. Given our estimates of the velocities of the major units, the critical cross over distance for refraction from the base of the basalt would be greater than 75 km. To detect changes in the basalt thickness across a region with enough resolution to identify a fault like contact by conventional refraction lines would be very difficult. We feel there are better methods to address this problem. One of these methods has already been done and another may have been done. Eaton's time term method is a refraction technique which incorporates the three dimensionality of the problem. We feel that this work is a significant beginning to looking at the detailed structure of the area and suggest that his final report be given strong consideration. We also feel there must exist reflection data for the area around Rattlesnake #1 well. It is inconceivable that a 10 km deep well

would be drilled without some reflection work being done in the area. We suggest that the company drilling the well be contacted about reflection data that may be available for the area. If these data are not available or are not extensive enough, we suggest vibroseis as a technique with unique potential for these types of structural studies. Since we do not have special expectise in vibroseis we suggest contracting with another organization for this type of investigation.

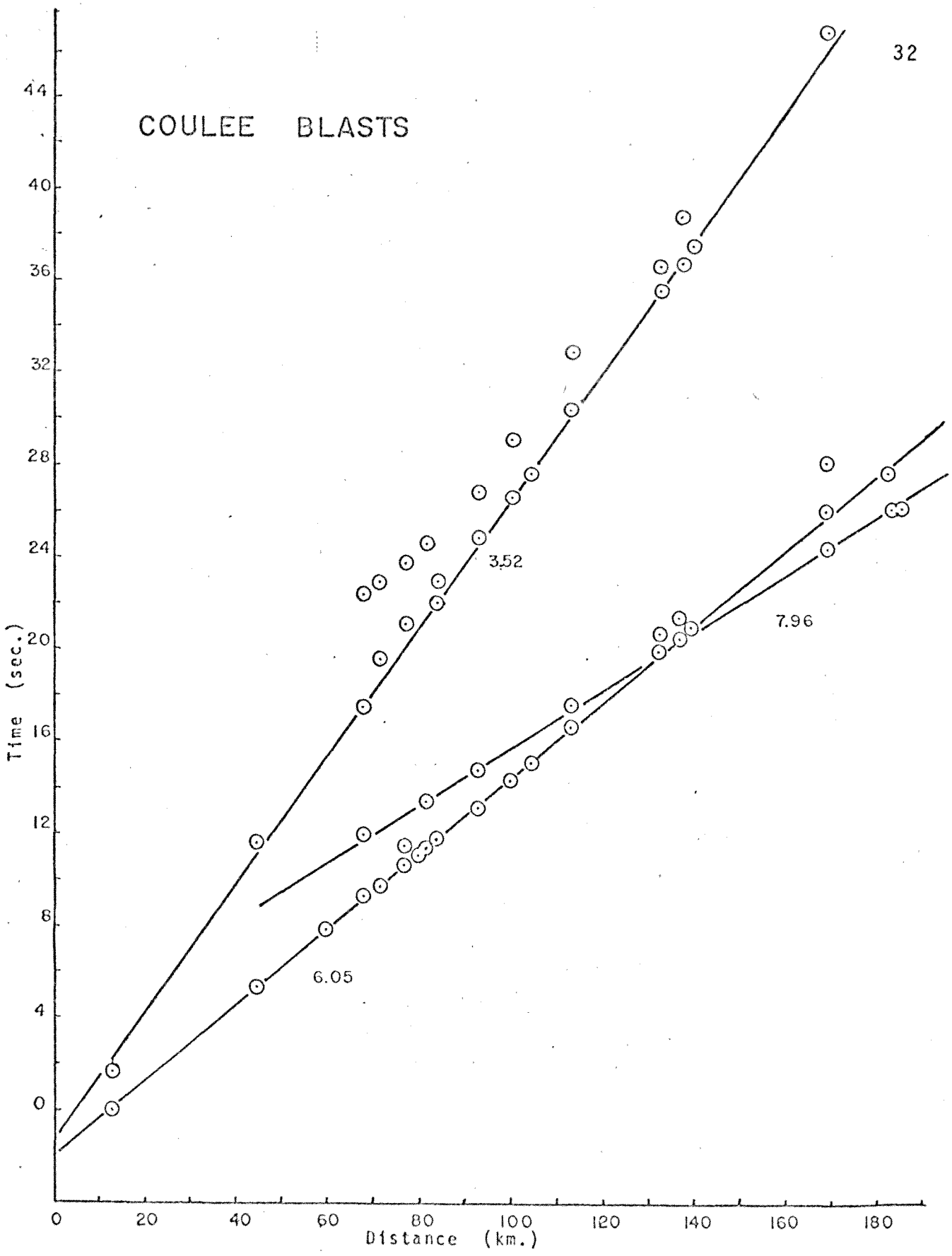


Figure 10. Time - Distance plot of major arrivals from a large quarry blast near Grand Coolee dam.

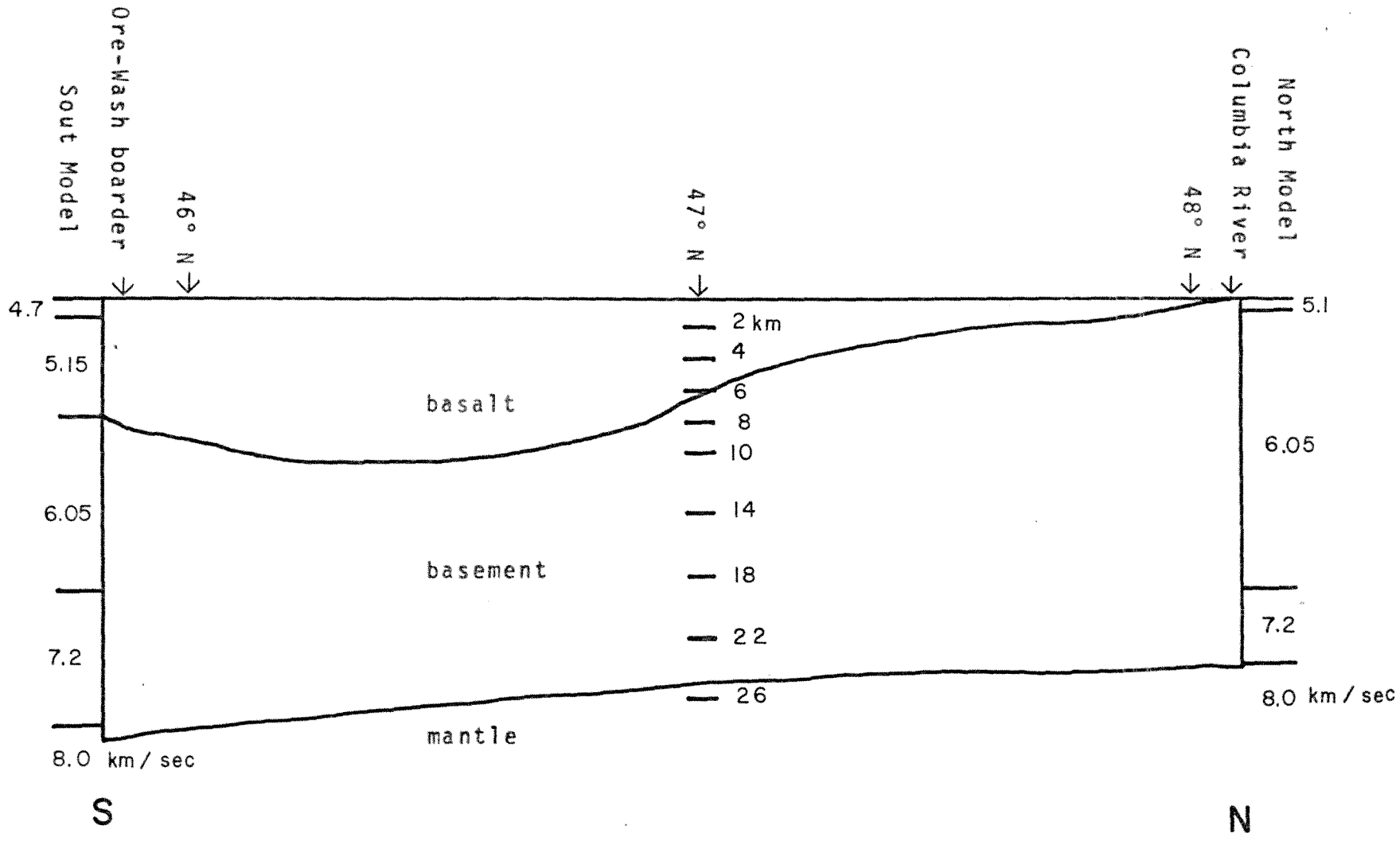


Figure 11. Idealized N-S section from time-term analysis. (Southern part is from Eaton's preliminary report)

TABLE 2. Eastern Washington Velocity Models.

| | V (km/sec) | DEPTH |
|---|---|---|
| A. Old Routine Model | | |
| | 3.70 | 0.0 |
| | 4.70 | 0.8 |
| | 5.10 | 1.5 |
| | 6.10 | 7.5 |
| | 6.80 | 15.0 |
| | 8.00 | 28.0 |
| B. North Model | | |
| | 5.1 | 0. |
| | 6.05 | 0.5 |
| | 7.20 | 19.0 |
| | 8.0 | 24.5 |
| C. South Model | | |
| | 3.7 | 0.0 |
| | 4.7 | 0.8 |
| | 5.15 | 1.2 |
| | 6.05 | 7.5 |
| | 7.20 | 19.0 |
| | 8.00 | 28.0 |

## Magnitude and Attenuation Study

Because a coda length-magnitude relationship has never been established using the local magnitude definition by Richter for eastern Washington, we have been using the relationship typically used for California events. Since we felt it was important to determine the appropriate scaling relation specifically for eastern Washington, we set out to do this during the past year. Two methods have been used which give similar results. One involves using the permanent telemetry stations in eastern Washington and a pseudo-Wood-Anderson response by obtaining well calibrated recordings on magnetic tape of earthquakes, while the other involves using a single standard Wood-Anderson seismograph to obtain recordings. These techniques are described and compared below.

Pseudo-Wood-Anderson. Twelve events that occurred during January to March 1977 in the Chelan area were used to study magnitude determination (Table 3 ). All these events were recorded on analog FM tape as part of the Chelan area study and then digitized by a 12-bit digitizer of the Varian computer. The maximum zero to peak trace amplitudes of the digitized seismograms were measured and the frequency estimated by counting peak in a time domain. The amplitude was then multiplied by the inverse response of the recording system giving the true ground displacement. The corresponding Wood-Anderson maximum trace amplitude was calculated by using the response curve of the Standard Torsion Seismometer (To = 0.8 sec, V = 2800, h = 0.8) (Figure 12). This can be done by assuming the frequency of the maximum amplitude is the same in both systems, because the frequency range falls within the flat region of W-A response curve. The hypocentral distance rather than epicentral distance was used when Richter's (1958) local magnitude formula was applied because the

proximity of events and stations. A correction of $\Delta M = +0.25$ was also applied because all the seismometers were vertical component (Eaton, 1970) and Richter's formula is designed to be used with horizontal component instruments. An example of the procedure is shown in Table 4 . The final magnitude results was plotted versus average coda length and a best git line drawn through these data points (Figure 13). The line fit through the data is our estimate of the magnitude-coda length relationship.

It matches very closely the one used in western Washington determined by Robert Crosson (1972). The previously used relationship is illustrated by the dashed curve determined by the USGS for central California and has a more gentle slope and a larger vertical intersection.

True Wood-Anderson. Wood-Anderson instruments were installed at Entiat, Washington in the latter part of January 1977, to record small local earthquakes for better magnitude determination. This location was chosen because of the relatively higher seismic activity during the late part of 1976 in this general area.

We experienced large drift problems of the instruments, and because of the high magnification, data gathering was intermittnet for the first month and a half. Originally, we hoped to record at 10,200 magnification; however, due to the drift problem we reduced the magnification to 5,600. At this magnification, we should be able to see most earthquakes of magnitude 2.5 within 50 km of Entiat.

We have recorded five events on the Wood-Anderson instruments which were also recorded and located on the central Washington array. A comparison of coda length and Wood Anderson magnitude is shown in Table3 and Figure13 . Most of the earthquakes listed in Figure 13have a epicentral distance of less than 25 km. This short distance creates a problem in computing a true

Richter magnitude (Gutenberg and Richter, 1942). We will probably record at this location through the fall before moving the instruments to a location on the Hanford Reservation Area.

As can be seen in Figure 13 there is fairly good agreement between the magnitude estimations determined by the two methods and an empirical scaling relation can be determined fairly well from these data. The fact that this relation is essentially the same as that for western Washington even though the geology and average earthquake depth are quite different is amazing. We do not have an explanation for this result other than a combination of effects are involved which fortuitously result in similar scaling laws.

The earthquakes reported on in the seismicity section of this report include this new magnitude-coda length relationship in their reported magnitudes and should supercede the events listed in our previous quarterly reports. We feel that these magnitudes more closely reflect true local magnitude as defined by Gutenberg and Richter (1946).

Using our revised magnitude relation we may estimate the magnitude threshold over which all events are located. If the log of the cumulative number of earthquakes greater than a given magnitude is plotted against that magnitude the points should fall along a straight line whose slope gives a relationship between the number of small events versus large ones in a given time period. This slope or "b" value is usually around -.7 to -.9 for tectonic areas characterized by large through going faults and large tectonic structures. Values for b from -1.0 to -1.5 are characteristic of areas with smaller scale tectonics such as volcanic or swarm areas. A "b" value plot for the Hanford region is given in Figure 14 for the period April 1975 through March 1977. The square outline in Figure 6 shows the areal

extent of the data for this plot. All known or suspected explosions were removed before plotting. The slope of this curve is about -.8 though the fit is not excellent. Note that for magnitudes less than $M_L$ = 2.0 the curve begins to deviate from the linear portion indicating that some events below this magnitude are being missed. For example at $M_L$ = 1.8 20 % of the events in that quarter magnitude range are being missed while half of the events are being missed at $M_L$ = 1.5. This gives a good check on the locatability of events in the Hanford area.

Seismic energy attenuation. From the digitized records in the period of January to March, 1977, 15 earthquakes and three blasts were selected. A standard data processing technique was applied to all of the selected events. The first S wave arrivals were picked by inspection, and then checked by the travel time obtained from the velocity model and locations. A rectangular time window of 1.024 sec long, 128 samples correspondingly, was then applied to the S arrivals. The S arrivals picked were assumed to be direct arrivals since the crossover distance for the second layer S arrivals is 148.8 km for a surface source and the epicentral distances of the events studied fall within this range (Figure 10).

The Fourier amplitude density spectra of the signals were calculated by using a library routine SPEC in the Varian computer, and the instrument responses were removed. To obtain a spectral noise estimate, a section of record preceding the P-wave onset for each event was analyzed using the same procedure. Beside the effects of source and medium complexities there are other factors which will cause the large variance of the spectra such as the long term drift of the recording system, the impulsive nature of the signal (i.e. they are non-stationary signals), the length of the time window and the additive background noise. Therefore, a three points smoothing window was

applied to the raw spectra in the sense of Hemming. A list of selected events and their locations are given in Table 5. Figure 15 shows a typical small event in the Chelan region. Examples of the raw spectra and the smoothed spectra are shown in Figure 16.

These data are being used to estimate the attenuation characteristics of the region. There are two mechanisms affecting attenuation, frequency independent or geometrical attenuation and frequency dependent or anelastic attenuation. We will deal with these separately.

First, a conventional frequency independent attentuation relation is assumed:

$$A \alpha r^{-n}$$

where A is the amplitude of the ground displacement at a hypocentral distance r. The value n is estimated from the observed data. Rewriting this in logarithmic form:

$$\log A \alpha -n \log r$$

Since many additional factors affect the observed A values, a direct plot of these values for any frequency versus r cannot define a value for n. Therefore, a filtering procedure was applied to the smoothed spectra.

The amplitude density spectra were divided into three groups: 3-9 Hz, 10-17 Hz, 18-24 Hz. The mean value for each groupwas calculated and only those values which had a signal to noise ratio larger than two were retained. From Figure 16 we see these values represent three different regions in the log-log plot of the Fourier spectrum. The low frequency range (3-9 Hz) is within the approximately flat region of the spectrum the value of which is proportional to the seismic moment. Although the spectrum in this range may be dependent upon the long term drift of the recording system and the time window length of the signal, the variance can be suppressed by applying a

smoothing window in frequencies higher than that corresponding to the half length of the time window.

Most of the log-log plots of the observed spectra showed corner frequencies around 10-15 Hz. Some of the stations showed a spectral peak around this frequency range causing a large variance of the n value. Hence, the amplitude density in the intermediate frequency range provides little help for determining the attenuation.

Generally, the signal to noise ratio in the high frequency range (18-24 Hz) is larger than two. The directivity of a propagating source is the most important cause of the large variance of the amplitude density in this frequency range (Ben-Meneham, 1961). For earthquakes with small magnitude, this effect is not very prominent. Additionally, the amplitude density in this frequency range corresponds to the flat part of the acceleration spectrum. This is advantageous because this portion of the acceleration spectrum represents the maximum acceleration over the duration of the signal.

In order to eliminate the effects of the unknown directivity and the radiation pattern of each earthquake, the stations were selected so that at least two were aligned with the epicenter or so that the difference between the azimuthal angle was approximately 90°. Based upon the above discussions, the n values were estimated for the low and high frequency ranges. The average n value for the low frequency range was $1.400 \pm 0.281$, and $1.852 \pm 0.447$ for the high frequency range. Table 6 shows the events and stations that were used and the n value for each station pair. These results suggest that the attenuation is frequency dependent, which is what one would expect if the crust is anelastic. In the near future an attempt to estimate the quality factor Q (which describes the anelasticity) in the crust for this region will be made.

TABLE 3 List of events used to determine magnitude.

PSEUDO - WOOD-ANDERSON

| DATE | HRMN | SEC | LAT | LONG | DEPTH | $M_L$ | ERROR | CODA LENGTH | ERROR |
|---|---|---|---|---|---|---|---|---|---|
| 77 01 01 | 21 56 | 5.30 | 47- 45.34 | 120- 40.03 | 3.70 | 1.84 | 0.1 | 31.5 | 6 |
| 77 01 02 | 16 50 | 15.28 | 47- 42.59 | 120- 13.06 | 5.40 | 1.76 | 0.4 | 29.0 | 4.3 |
| 77 01 16 | 13 31 | 54.19 | 47- 43.33 | 120- .74 | 8.00 | 1.00 | 0.05 | 13.3 | 2 |
| 77 01 20 | 21 11 | 37.76 | 47- 46.05 | 120- 3.22 | 4.37 | 1.40 | 0.2 | 23.3 | 3.1 |
| 77 01 28 | 11 19 | 42.47 | 47- 38.21 | 120- 8.84 | 6.20 | 1.50 | 0.4 | 29.6 | 2.1 |
| 77 01 31 | 19 23 | 11.96 | 48- 8.89 | 119- 9.61 | 1.50 | 1.79 | 0.24 | 37.2 | 6.5 |
| 77 02 11 | 03 06 | 9.54 | 47- 40.30 | 120- 19.64 | 8.00 | 1.39 | 0.2 | 33.7 | 2.4 |
| 77 02 17 | 21 33 | 25.47 | 47- 39.93 | 120- 21.42 | 3.00 | 1.31 | 0.18 | 20.5 | 1.5 |
| 77 02 23 | 04 28 | 20.23 | 47- 41.34 | 120- 2.84 | 7.13 | 1.48 | 0.22 | 28.8 | 1.0 |
| 77 03 08 | 04 45 | 11.19 | 48- 30.93 | 120- 24.79 | 1.50 | 2.55 | 0.13 | 59 | 8 |
| 77 03 10 | 10 44 | 53.87 | 47- 39.03 | 120- 12.32 | 7.42 | 1.76 | 0.23 | 37.5 | 2.3 |
| 77 03 15 | 22 36 | 36.78 | 47- 39.30 | 120- 12.05 | 7.30 | 1.01 | 0.2 | 17.3 | 1.6 |

TRUE - WOOD-ANDERSON

| | | | | | | | | | |
|---|---|---|---|---|---|---|---|---|---|
| 77 03 08 | 04 45 | 11.19 | 48- 30.9 | 120- 24.8 | 1.5 | 2.7 | | 57 | 6.2 |
| 77 05 09 | 23 50 | 43.48 | 47- 43.4 | 120- 13.4 | 14.3 | 2.5 | | 60 | 4.9 |
| 77 05 12 | 09 48 | 14.94 | 47- 40.2 | 120- 07.5 | 0.1 | 2.0 | | 44 | 14.3 |
| 77 05 17 | 04 13 | 08.19 | 47- 39.1 | 120- 23.4 | 0.1 | 1.8 | | 36 | 4.7 |
| 77 06 11 | 16 24 | 32.00 | 47- 40.5 | 120- 13.1 | 7.2 | 2.1 | | 41 | 3.5 |

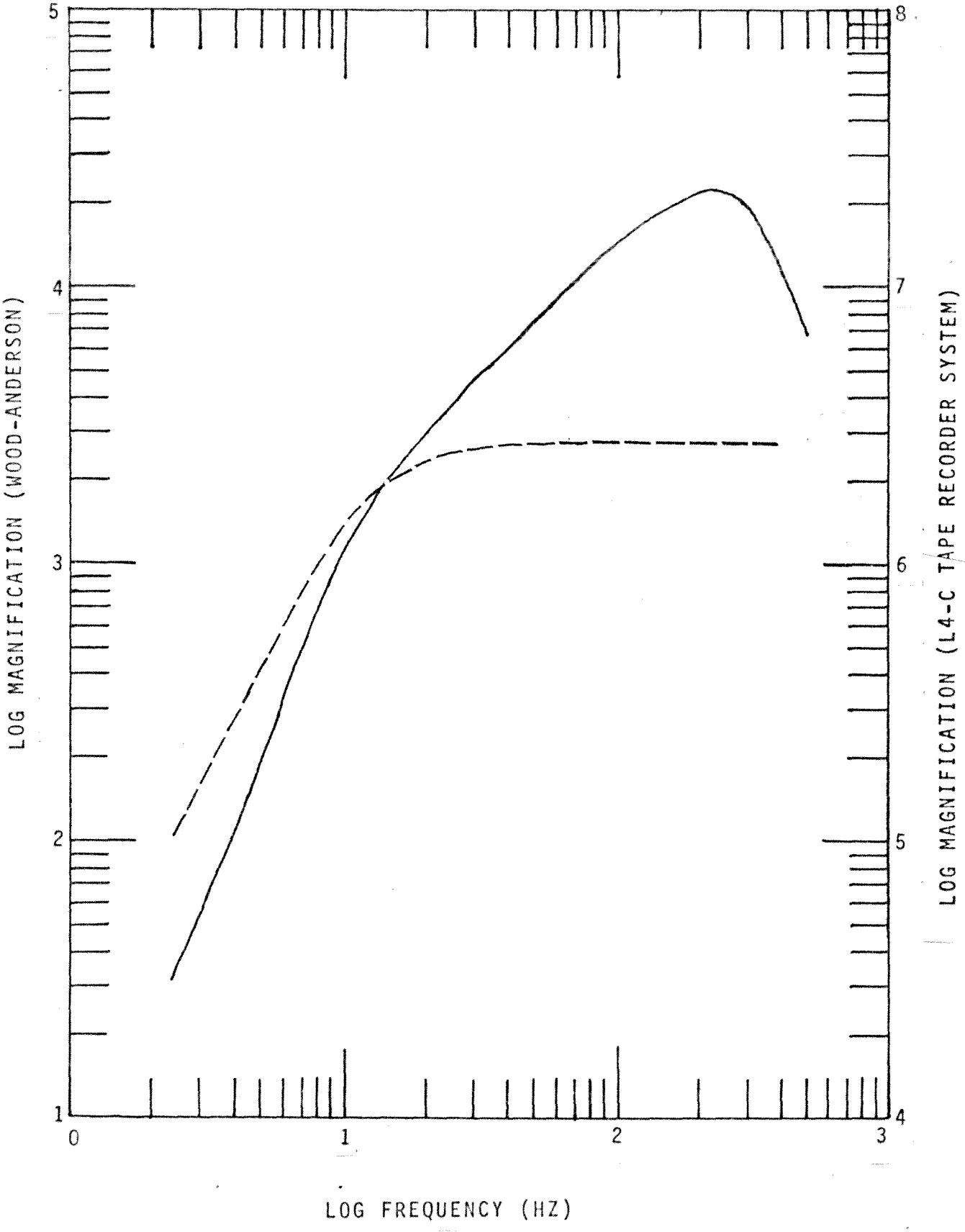


Figure 12. Calibrated instrument responses for magnitude study. Solid line is Wood-Anderson, dashed is telemetry system.

TABLE 4. Example of the procedure of magnitude determination, stations with asterisk have not been used because of large deviation. The average magnitude is 1.23 ± 0.22, then +0.25 has been added with reason given in the text.

| DATE | HM | STA | M Amp (m.m.) | f (hz) | In. Resp $x10^{-5}$ | Ground Motion $x10^{-5}$mm | W-A Resp | W-A Amp $x10^{-2}$mm | log A | Δh (km) | -log $A_o$ | $M_L$ |
|---|---|---|---|---|---|---|---|---|---|---|---|---|
| 77 02 23 | 0428 | WAT* | 32.5 | 12.4 | 2.992 | 9.724 | 2792 | 27.149 | -0.57 | 9.7 | 1.49 | 0.92 |
| Depth = 7.13 km | | CHB | 29 | 14 | 3.125 | 9.063 | 2794 | 25.321 | -0.60 | 15.2 | 1.60 | 1.0 |
| | | WEN | 26 | 12.4 | 2.258 | 5.871 | 2792 | 16.391 | -0.79 | 22.1 | 1.78 | 0.99 |
| | | FLP | 20 | 15 | 1.923 | 3.846 | 2795 | 10.749 | -0.97 | 34.5 | 2.28 | 1.31 |
| | | EPH | 14 | 10 | 1.070 | 1.496 | 2787 | 4.175 | -1.38 | 50.5 | 2.61 | 1.23 |
| | | SAN | 11.5 | 15 | 3.401 | 3.911 | 2795 | 10.932 | -0.96 | 48.5 | 2.57 | 1.61 |
| | | WIL* | 19 | 14 | 3.472 | 6.597 | 2794 | 18.431 | -0.73 | 77.2 | 2.87 | 2.14 |
| | | DYR* | 7 | 3.1 | 13.831 | 9.682 | 2659 | 25.744 | -0.59 | 37.3 | 2.35 | 1.76 |

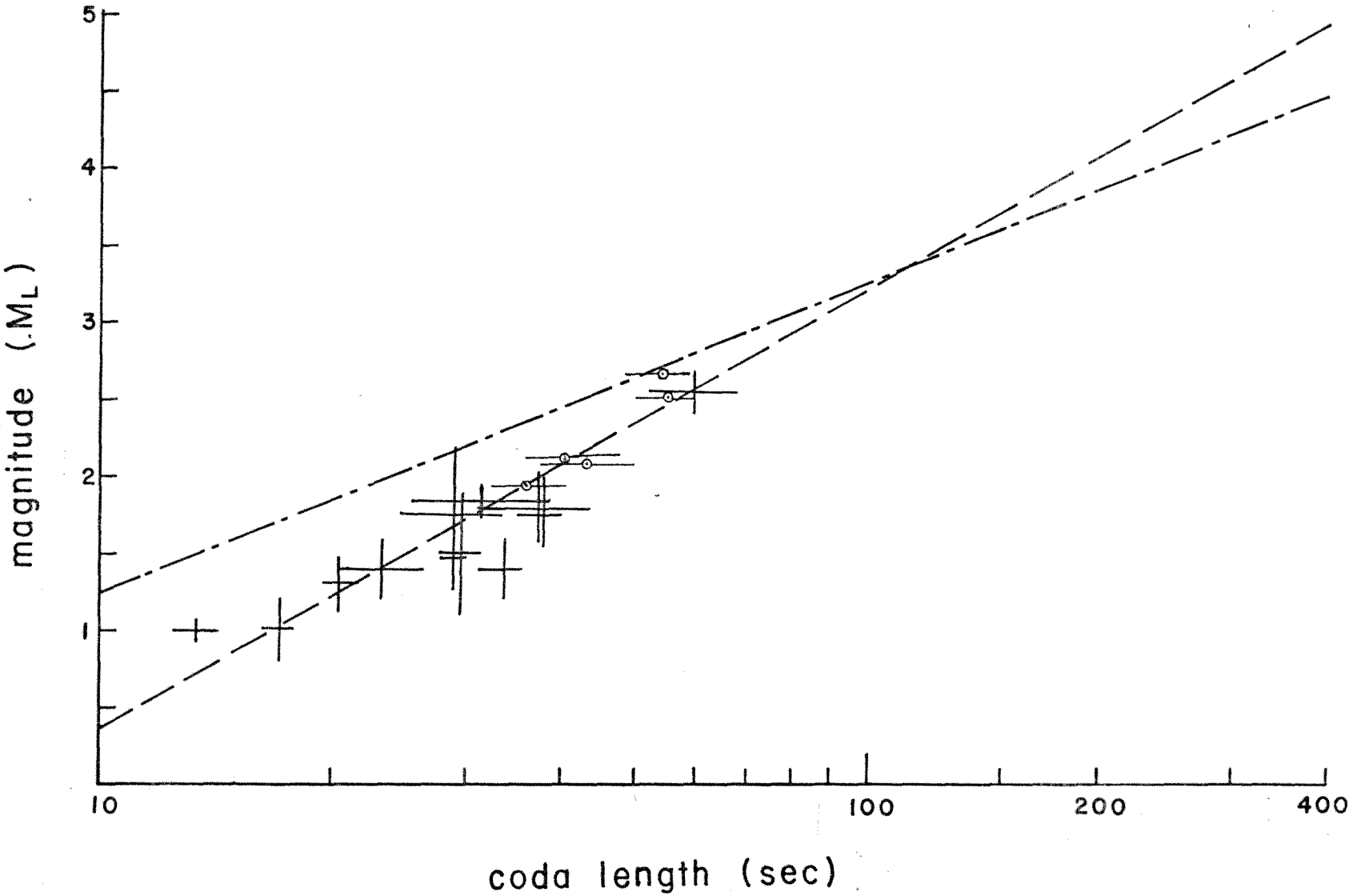


Figure 13. Empirical relation between coda length and magnitude in eastern Washington. Solid curve is best fit through the pseudo Wood-Anderson (crosses) and the true Wood-Anderson (circle and bar) points. Dashed curve is California relation.

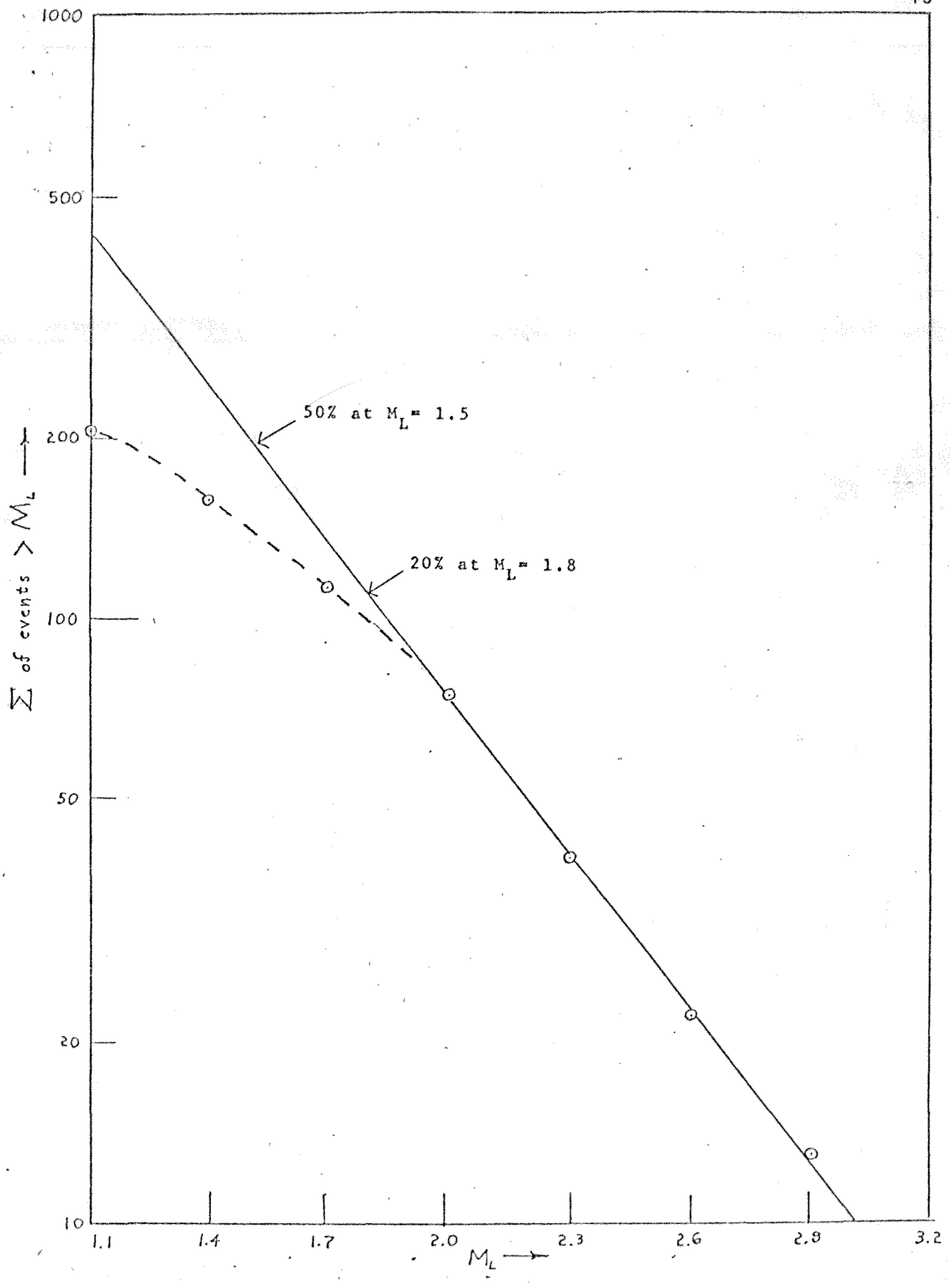


Figure 14. Log N verses M or "b" value plot for U.of W. located earthquakes in Hanford area. Slope is -0.8.

## Detailed Studies

There were two specific areas which were involved in detailed studies. The data from the Wooded Island swarm of 1975 has been analysed in some detail. An anisotropic velocity model is being used to relocate the earthquakes with the hope that the focal mechanisms will be more consistent. The area just south of Lake Chelan is also of some interest since it is the most seismically active area in the north central basin.

Lake Chelan study. The area around the south end of Lake Chelan has been known to be seismically active for some time. Rasmussen (1967) reports over 60 earthquakes centered in that region and felt during historic time. The largest of these was probably one in April, 1958 which was most strongly felt just north of Lake Chelan on the Columbia river and had a maximum intensity of VI$^{+}$. It is also possible that the large north Cascades earthquake of 1872 was centered in this area though much of the intensity data suggests an epicenter farther north.

During the years the USGS ran the Hanford seismic net over a dozen events were located by them in the Chelan-Entiat area even though their nearest station was over 60 km away. The University of Washington ran a single station near the town of Chelan from 1973 to 1975. Many local events were noted on this station though they could not be located and many were thought to be local quarry blasts. In 1975 with the expanded Hanford array several events per month were located in this region. In late 1976 two new stations were added to the area (ENT and WAT) and in early 1977 all the stations in this region began to be recorded on our portable array magnetic tape system such that improved timing and first motion picks were available. We report below the results of research thus far in this area.

From mid 1975 until March 1977 we have located 69 events in the general Lake Chelan area which are not blasts and which have well controlled hypocenters with time residuals, RMS value, less than 1/4 second. These events are plotted in Figure 17 . For the events in the immediate ENT-WAT area the average estimated error in epicenter is around 1 km and in depth is 1.5 km. For the events to the east near EPH and SAW the epicentral error is around 1.5 km while the depth is poorly controlled (error $\geq$ 5 km).

Figure 18 is a blow up of the ENT-WAT area where the symbols are a function of depth. The depth histogram shows that most of the events are around 5 or 6 km deep with few deeper than 10 km or shallower than 3 km. There appear to be no obvious line up of events from which a fault or controlling structure could be inferred. The group of events just to the east-south-east of ENT have a distribution of depths in no obvious pattern. Farther to the east lie a group of events which could be argued to line up roughly north-south extending almost to CBW. Another such north-south line up may extend north from ENT, and a possible roughly east-west line up may exist to the east of ENT. All of the above observations are quite tentative since there exists no strong evidence for any of the above line ups. We do feel that the rather confused distribution of hypocenters is real and not an artifact of the station distribution or location procedure.

In an attempt to make some sense from these data first motion plots have been made using the events which were well recorded on a number of stations including ENT and WAT. These events are shown in Figure 19 where all events are larger than $M_L$ = 1.5. The average epicentral error for these events is less than 1/2 km and depth error less than 1 km. Since no single event has enough first motion data available these nine events were composited onto one plot shown in Figure 20. It is obvious that no

single fault plane solution is possible from these data. The picture remains as confused as ever. We hope that the new stations installed July 1 will help solve this problem and plan to put our portable network in the area this fall if need be.

Details of Microearthquake Swarms - Wooded Island

We have examined the effect of the layering of the basalts (anisotropy) on seismic energy propagation in an effort to explain questionable results from the standard analytical tool of Wadati plots. Our results show that the medium at Wooded Island must indeed be considered as anisotropic (transversely isotropic) when attempting to locate earthquakes from a distance of no greater than a couple hypocentral depths. We are presently developing a technique to locate earthquakes in such a medium in an attempt to better resolve details of the spatial distribution (i.e. fault planes, if they exist) of the swarm at Wooded Island.

We chose events with three or more pickable shear phases and attempted to construct Wadati plots. The basic assumptions of Wadati was that P and S take the same path and that the elastic parameters didn't vary over the path. If one plots P time versus S-P time, and the above assumptions are true, the slope of the best fitting straight line yields the ratio of the compressional to shear wave velocities. Figure21b shows the $V_p/V_s$ values obtained from Wadati plots by the weighted least squares technique ranged from 1.6 to 2.6 for Wooded Island events. Compare these results to those for events in the Lake Chelan area which cluster tightly about 1.72 (Figure21a) which is close to the average measured for most rocks.

If a medium is anisotropic the assumptions of Wadati are not valid. Therefore, if the medium at Wooded Island can be shown to be anisotropic, the failure of the Wadati plots to converge on a single value of $V_p/V_s$ characteristic of the medium may be explained.

To examine in particular the medium at Wooded Island, we obtained the elastic parameters for competent basalt and interflow material from the elastic properties log for the well DC-1 on the reservation. Using elastic wave theory, others have shown that the velocity of compressional and shear waves is highly dependent on angle of incidence to the axis of symmetry (i.e. perpendicluar to the layering). Others have also shown that there is a splitting of the shear wave energy into particle motion parallel (SH, horizontally polarized shear) and perpendicular (SV, vertically polarized shear) to the layering. In addition to this splitting, the SV wavefront, or picture of the energy discontinuity at a particular time, is not a simple smooth surface, but contains a cusp. Figure 22 shows the wavefronts at T = 1 sec (solid line) and T = 2 sec (dashed line). Note that depending on the source-receiver geometry anywhere from 2 to 5 direct body phases may be observed.

We are currently examining seismograms from the 1975 Wooded Island swarm to determine if the multiple shear wave arrivals predicted by the anisotropic theory are indeed observed. If the seismograms indicate that the medium does split and propagate the theorized body waves, we should proceed to relocate the earthquakes of the Wooded Island 1975 swarm as recorded by the small portable array. Although others have studied propagation of the elastic waves in anisotropic media, no one, to our knowledge, has addressed the problem of hypocenter determination in such a medium.

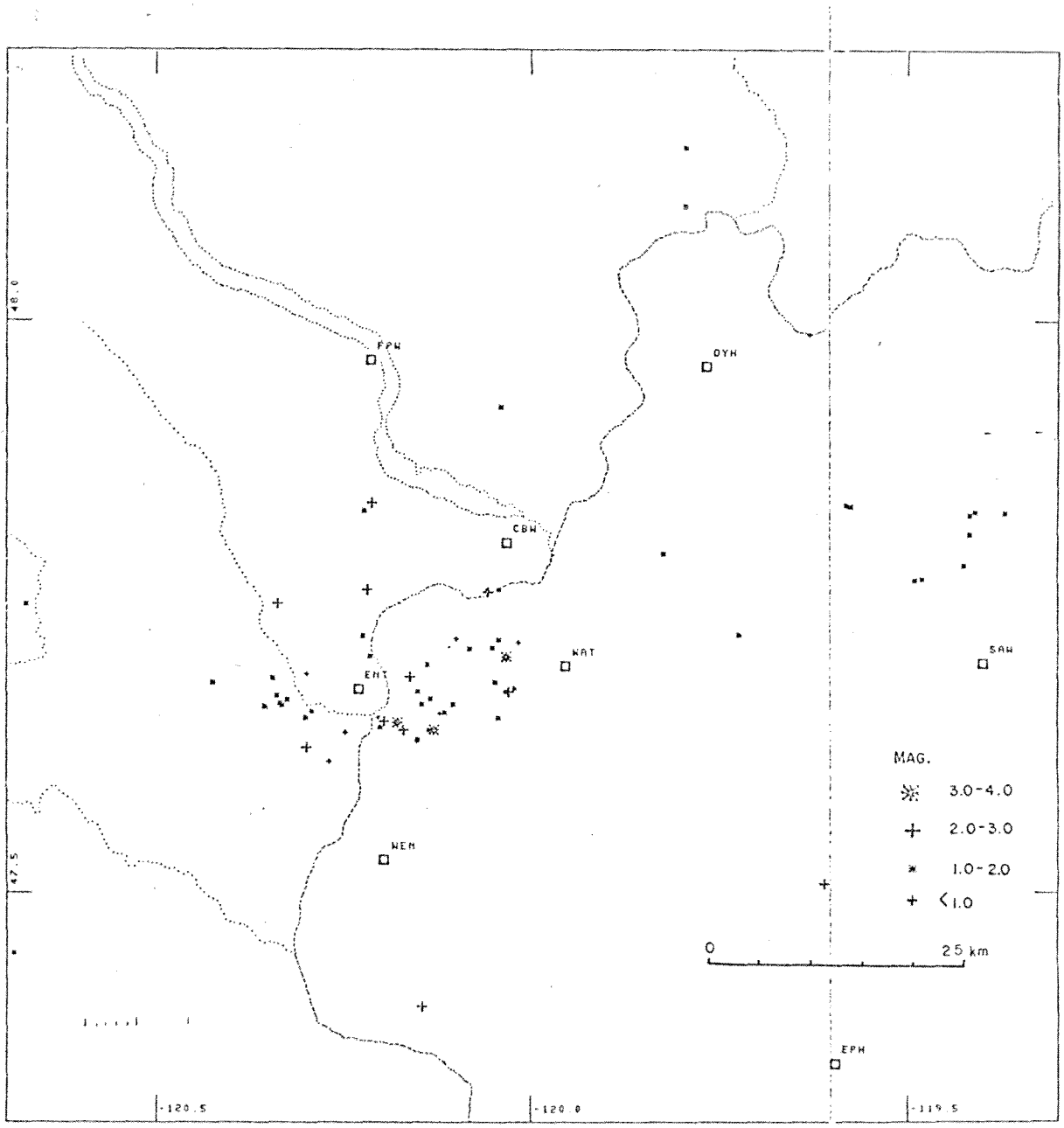


Figure 17. Map of all located earthquakes in the southern Lake Chelan area from July 1975 to March 1977.

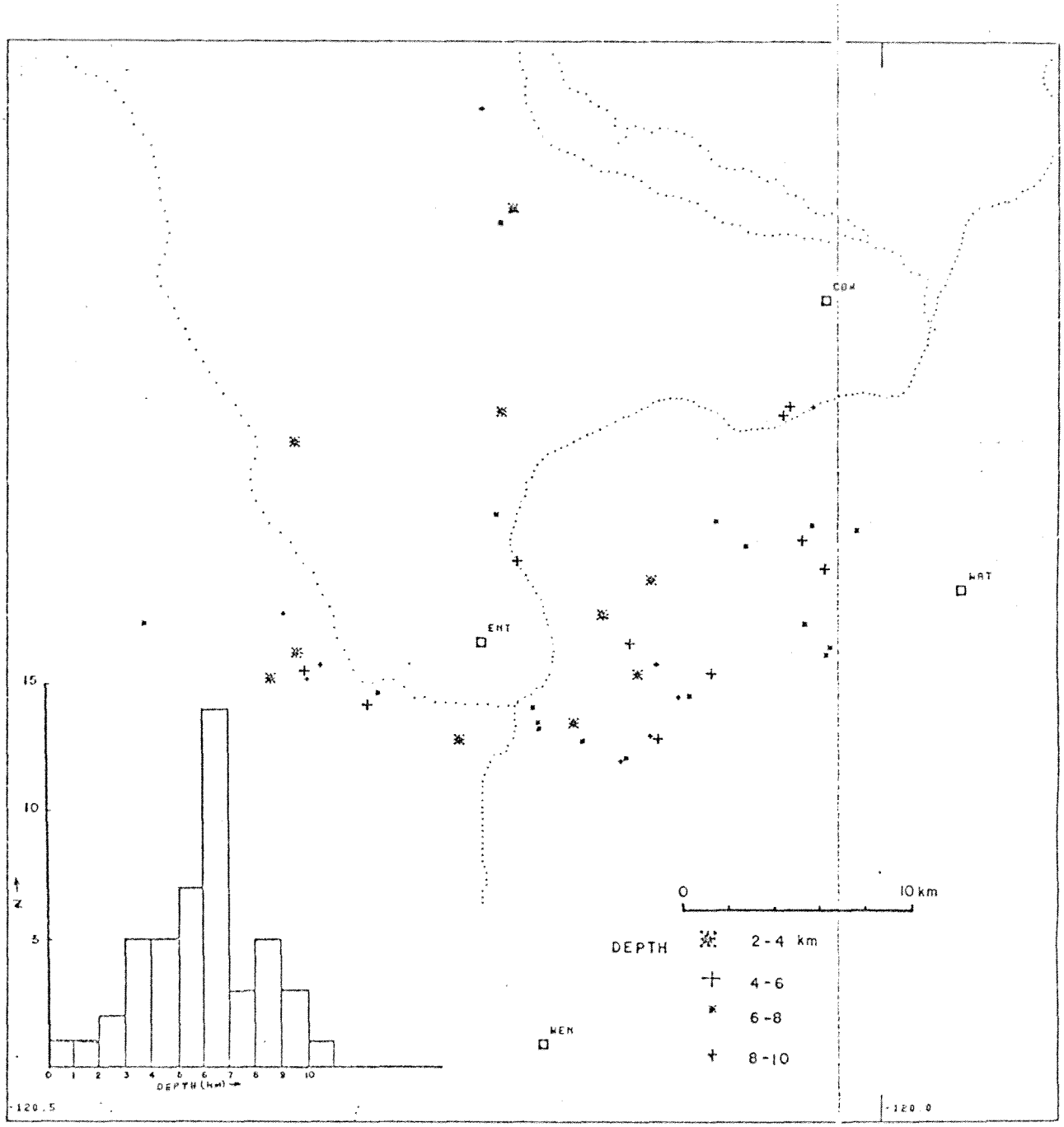


Figure 18. Blow up map of the ENT-WAT area south of Lake Chelan with the earthquake symboles as a function of depth.

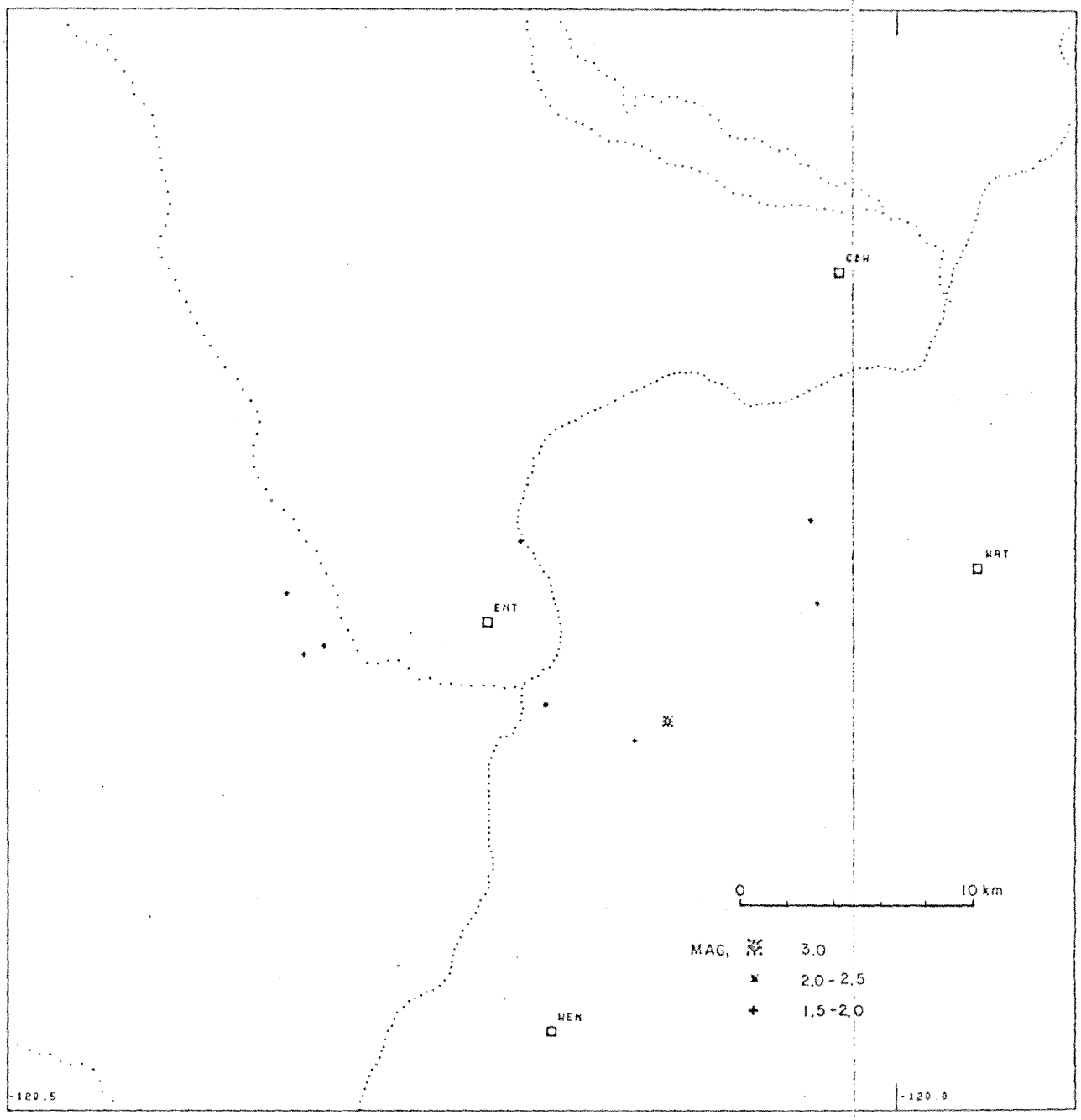


Figure 19. Earthquakes south of Lake Chelan located after ENT and WAT were installed. These events are larger than $M_L$ = 1.5 and were used for the first motion plot of fig.20.

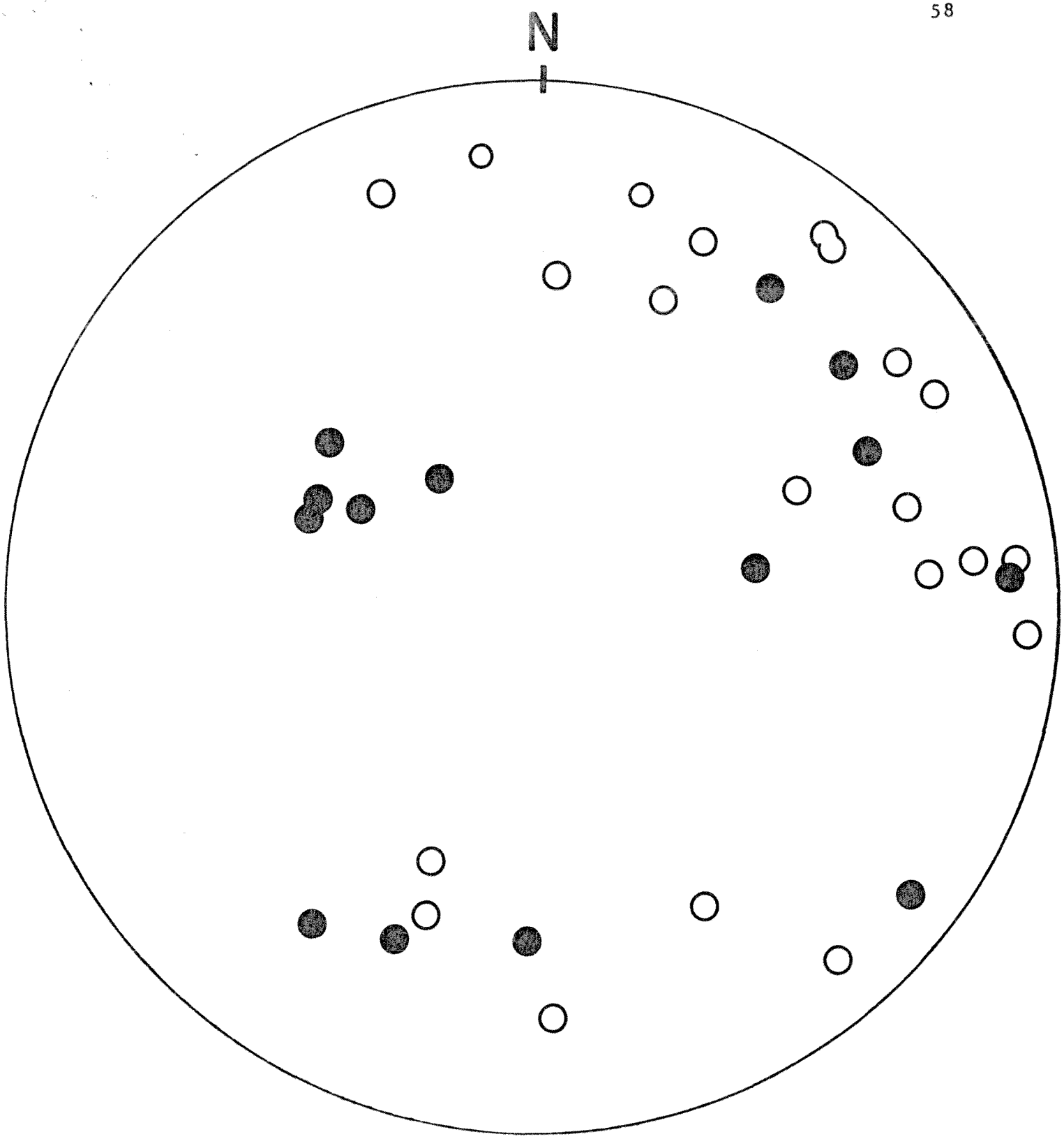


Figure 20. First motion plot for 9 earthquakes in WAT-ENT area. Solid is compression and open is dilatation. No single fault-plane solution can be fit to these data.

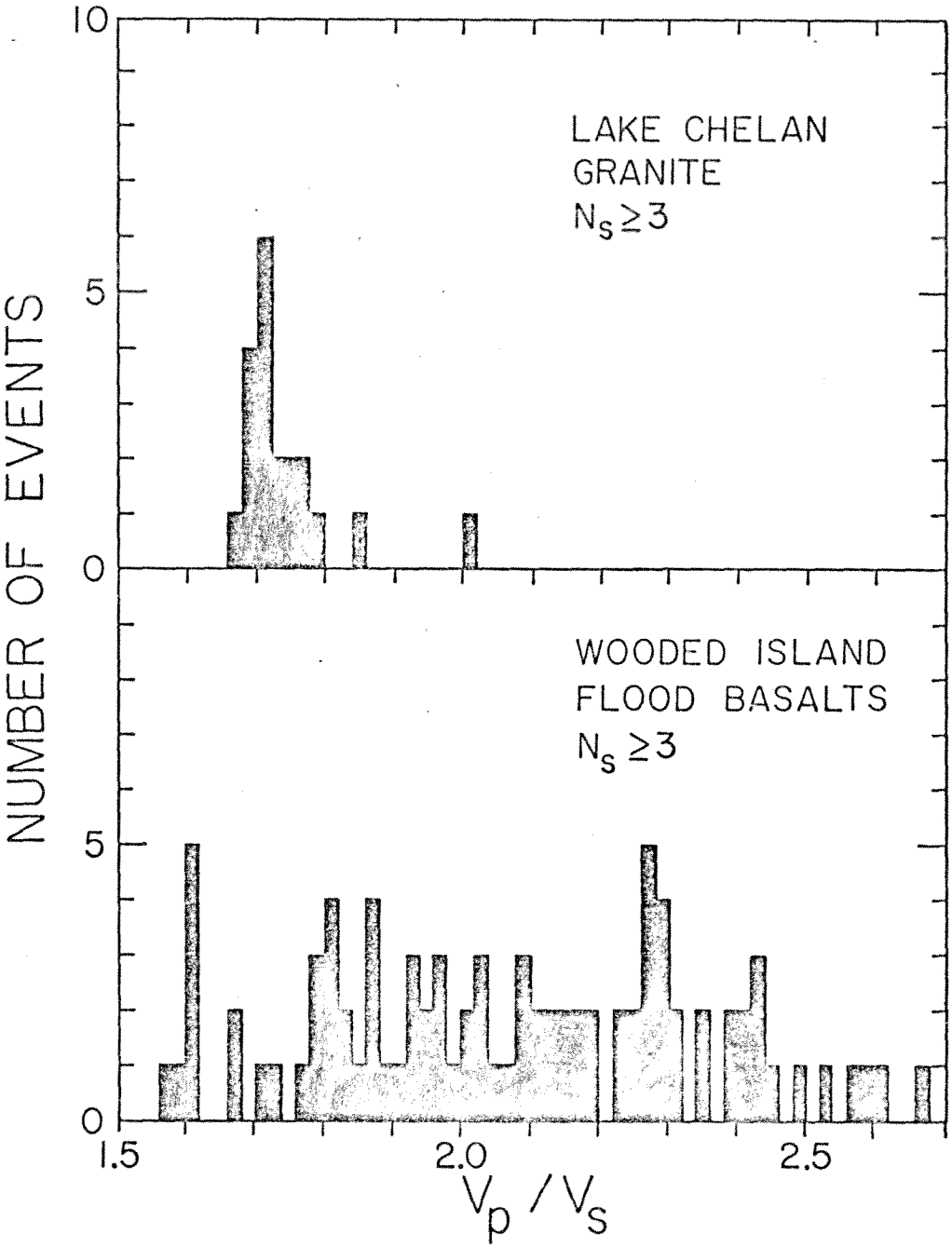


Figure 21 Histograms of $V_p/V_s$ from results of Wadati plots.

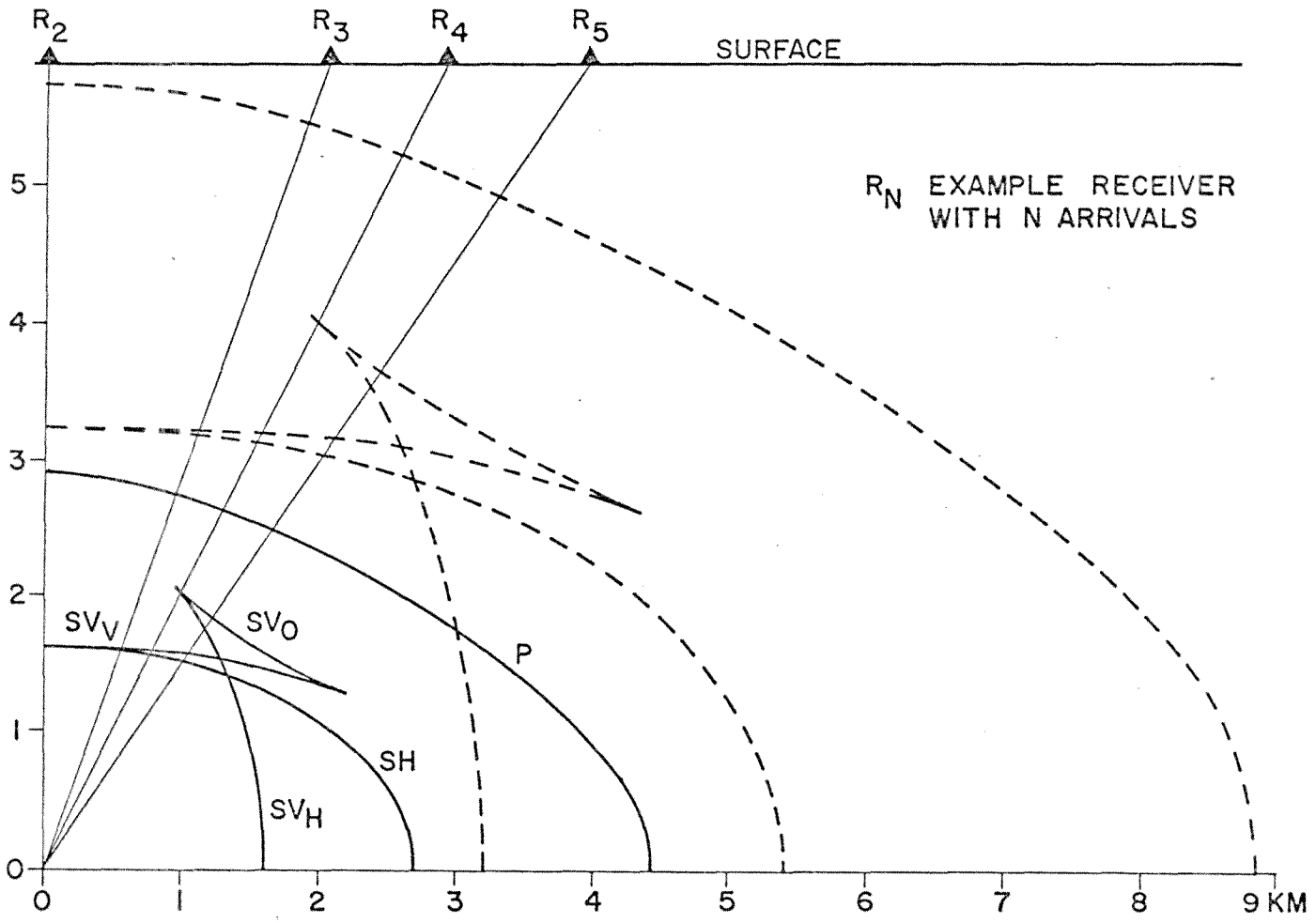


Figure 22 Wavefronts in a transversely isotropic (anisotropic) medium calculated using elastic parameters from well DC-1. Solid lines, T = 1 sec.; dashed lines, T = 2 sec.

Tiltmeter Experiment

The two kinemetrics TM-1 biaxial borehole tiltmeters were verified to be in good working order by attaching them to a seismic pier. Further testing involved a comparison with the tera-technology servo accelerometers on the same seismic pier. Tilts measured by both the kinemetrics and tera technology instruments were of similar magnitude, but noise conditions prevent a more detailed calibrating and test.

Since the kinemetrics tiltmeters are to be installed in remote locations, a telemetry system for each instrument was constructed to send the data to the University of Washington over the telephone lines. The transmitter multiplexes each component of tilt; digitizes the reading to 12 bits of resolution; then frequency shifts a 440 Hz voltage controled oscillator. The receiver decodes the F.S.K. from the phone line using a phase locked loop discriminator. The digital word is reconstructed by using another P.L.L. to recreate the transmitter's clock. The clock demultiplexes each tilt component to monitored continuously on a mult-channel strip chart recorder. Each tilt component is sampled once every 4 seconds. By using an inverter, two 2.5 volt, 1000 amp- air cells will power both a tiltmeter and its transmitter for about 1/2 year. C-MOS integrated circuits and a C-MOS A/D converter kept power dissipation in the transmitter to a minimum. The transmitter and inverter are housed along with the tiltmeter electronics in the original kinemetric weather proof box. The only external connections are the power and phone lines.

The transmitter was tested for environmental stability. Long term testing done at $-2^{o}C$ showed no functional failures and an acceptable VCO

drift of 4 Hzx from its room temperature center frequency. Short term high temperature test at about 50°C showed no functional failures and acceptable VCO drift.

The use of bubble-type tiltmeters such as those provided by the U.S. Geological Survey for this project is a subject over which there is considerable controversy at this time. Results from tiltmeter arrays in California show that there is considerable variation in signals depending on the local site conditions. In addition, some instruments appear to be noisy and it is not clear if the problem is in the instruments, or in the site conditions. To make tilt observations at Wooded Island we feel it is absolutely necessary to first have a direct measure of the instrument calibration and drift. Since the capabilities of these instruments exceed the kinds of tilt controlled environments available in a laboratory, or even on our seismic pier, we plan to install the two instruments side by side in the field to make a direct comparison between them. If they track satisfactorily, one of the instruments will then be moved to a more distant site.

Since there is only one phone drop with only one channel open, one of the transmitters and receivers is going through minor modifications to allow both components of both tiltmeters to be multiplexed together. Cycle time will be doubled to 8 seconds. The tiltmeters should be installed by early July and functional soon afterwards.

References

Aki, K., 1969, Analysis of the seismic coda of local earthquakes as scattered waves, J.G.R. 74, 615-631

Ben-Meneham, A., 1961, Radiation of seismic surface waves from finite moving sources, B.S.S.A. 51, 401-435

Crosson, R.S., 1972, Small earthquakes, structure, and tectonics of the Puget Sound region, B.S.S.A. 62, 1133-1171

Eaton, J.P., 1976, Preliminary report on crustal structure from explosions and notes on earthquake distribution, preprint

Eaton, J.P., M.E. O'Neill, J.N. Murdock, 1970, Aftershocks of the 1966 Parkfield-Cholame, California, earthquake: A detailed study, B.S.S.A. 60, 1151-1197

Gutenberg, B., C.F. Richter, 1942, Earthquake magnitude intensity, energy, and acceleration, B.S.S.A. 32, 163-191

Hill, D.P., 1972, Crustal and upper mantle structure of the Columbia Plateau from long range seismic refraction measurements, G.S.A. Bull 83, 1639-

McCollon, R.L., R.S. Crosson, 1975, An array study of upper mantle velocity in Washington State, B.S.S.A. 65, 467-482

Pitt, A.M., 1971, Microearthquake activity in the vicinity of Wooded Island, Hanford region, Washington, U.S. Geological Survey open file report

Pitt, A.M., 1976, Preliminary summary of seismic activity in the Hanford region from July 1970 to December 1974, preprint

Richter, C.F., 1958, Elementary Seismology, San Francisco: Freeman and Co., Chapter 22